A Novel Microfluidic Device for Rapid and Efficient Airborne Bacteria Capture and Enrichment.

ARTICLE *in* ANALYTICAL CHEMISTRY · APRIL 2013

Impact Factor: 5.64 · DOI: 10.1021/ac400590c · Source: PubMed

analytical chemistry

Article

pubs.acs.org/ac

Microfluidic Device for Efficient Airborne Bacteria Capture and Enrichment

Wenwen Jing,[†,∥] Wang Zhao,[†,∥] Sixiu Liu,[†] Lin Li,[‡] Chi-Tay Tsai,[‡] Xiaoyong Fan,[§] Wenjuan Wu,*[,§] Jingyan Li,[†] Xin Yang,[†] and Guodong Sui*[,†]

[†]Department of Environmental Science & Engineering, Fudan University, 220 Handan Road, Shanghai, 200433, P.R. China, and Institute of Biomedical Sciences, Fudan University, Shanghai, 200433, P. R. China

[‡]Department of Ocean and Mechanical Engineering, Florida Atlantic University, 777 Glades Road, Boca Raton, Florida 33431, United States

[§]Department of Infection Control, Shanghai Public Health Clinical Center, 2901 Caolang Road, Shanghai, 201508, P. R. China

Supporting Information

ABSTRACT: Highly efficient capture and enrichment is always the key for rapid analysis of airborne pathogens. Herein we report a simple microfluidic device which is capable of fast and efficient airborne bacteria capture and enrichment. The device was validated with *Escherichia coli* (*E. coli*) and *Mycobacterium smegmatis*. The results showed that the efficiency can reach close to 100% in 9 min. Compared with the traditional sediment method, there is also great improvement with capture limit. In addition, various flow rate and channel lengths have been investigated to obtain the optimized condition. The high capture and enrichment might be due to the chaotic vortex flow created in the microfluidic channel by the staggered herringbone mixer (SHM) structure, which is also confirmed with flow dynamic mimicking. The device is fabricated from polydimethylsiloxane (PDMS), simple, cheap, and disposable, perfect for field application, especially in developing countries with very limited modern instruments.

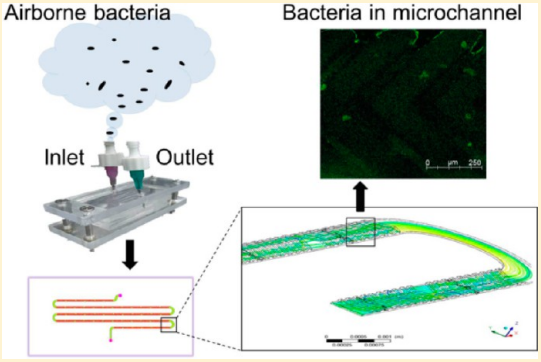

For the past decade, human beings are facing the serious reality of more emerging new infectious diseases and recurrence of old diseases.[1−5] Among all the infectious diseases, the respiratory infectious diseases are the most difficult ones for the control and prevention, which are also the ones causing public panic.[2,4] Compared with other diseases, the respiratory infectious diseases can spread rapidly in people, especially in the highly populated urban areas mainly because they are transported through air. Many respiratory infectious diseases are caused by bacteria, such as Anthrax, Lememia, Cholera, Malta fever, Tuberculosis (Pathogenic bacteria were *Bacillus anthracis*, *Yersinia pestis*, *Vibrio cholera*, *Brucella melitensis*, *Mycobacterium tuberculosis*, respectively). There are more than 20 different kinds of bacteria that can be transferred between people or animals.[6−9] Public health was threatened and damaged frequently, with no mention to the accompanying public panic and economic loss. Methodology for rapid or online detection of the airborne pathogens causing these diseases is essential for the disease control and prevention.[10,11]

Since most current pathogen analysis methods relies on the bioanalysis in aqueous medium,[12−18] the initial step for the airborne pathogen analysis is the efficient collection and transfer from air into the water medium. The general sampling methods for airborne pathogens include the natural sediment method and the machine sampling method. The natural sediment method was established by Koch in 1881. In this method, microbial particles in the air were settled by gravity on nutrient agar media before and after disinfection.[19] The machine sampling method, according to the principle of sampling, can be divided into sedimentation type, percussion, centrifugal impingement, filter type, electrostatic type, cyclone type, etc.[20]

There are different types of airborne collectors such as gravitational samplers, the Anderson sampler, AGI samplers, and centrifuge samplers.[2,21−24] Although many different types of samplers promote the development of air microbiology, so far fast and accurate sampling of the biological aerosol is still a difficult technical issue. So far, almost no sampling technique can ensure that the collected microbial specimen reflects the original state and can be directly used in bioanalysis.[19,20,25,26] Pathogen culturing is generally the necessary step before analysis, mainly because the concentration of the collected pathogen is too low for direct bioanalysis in the methods mentioned above. Culturing normally takes from 24 h, several days, to more than 10 days, which is too slow for rapid analysis, especially for the early disease warning and prevention situation. Some bacteria were in the state of viable but

Received: March 14, 2013
Accepted: April 17, 2013
Published: April 17, 2013

   dx.doi.org/10.1021/ac400590c | *Anal. Chem.* 2013, 85, 5255−5262

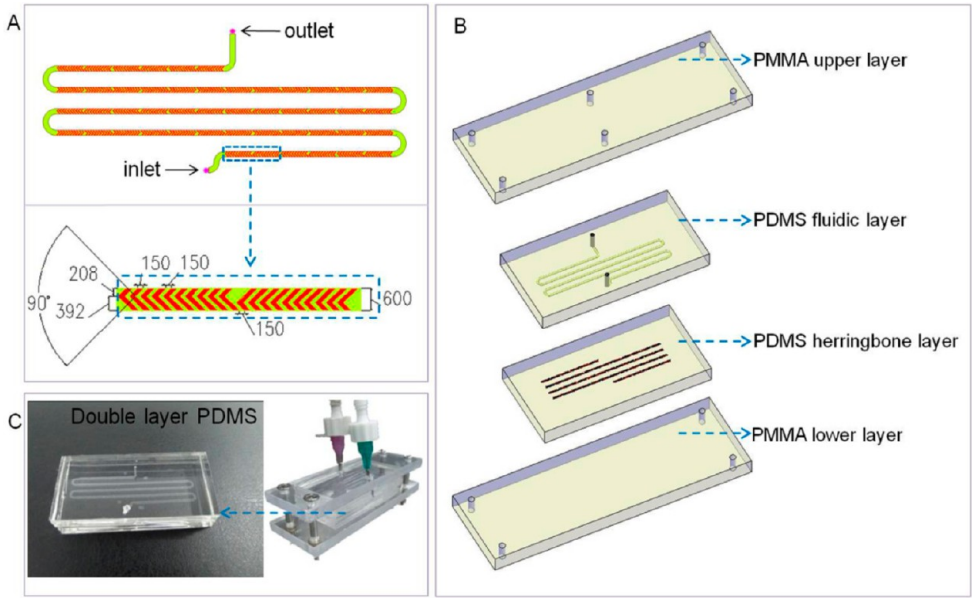

Figure 1. Structure of the microfluidic chip: (A) chip design and enlarged graph showing detailed structure of the microchannels (units, μm), (B) different components of the device, and (C) picture of the assembled chip and connectors.

nonculturable (VBNC) in natural environments.[26,27] Most pathogens are at submicrometer size, and the dimensions of the current samplers are at the millimeter or centimeter level. Because of the size difference, the water used to rinse/wash the samplers is generally too much, compared with the small amount of the pathogens collected in the samplers. Consequently, the concentration of the collected pathogens in the aqueous media is too low for direct bioanalysis.

In contrast, the microfluidics which handles liquid in the micrometer dimension, nanoliters in volume, might bring a new way to obtain adequate concentration pathogens in a relatively small amount of liquid.[9,28−30] Compared with the traditional system, there are improved reaction speed, mass transfer, and heat transfer inside the microfluidic chip, which makes it perfect for rapid bioanalysis such as protein analysis and gene analysis.[13,31−36] It is also highly economical with much less reagent consumption, suitable for a large scale deployment and field application.[33,37−39] Although many researches of cell capture by microfluidic chip have been reported,[40−43] most of them focused on tissue cells capture and rarely refer to airborne bacteria cells capture directly from the air. Herein we report a simple microfluidic device which is capable of fast and efficient airborne bacteria enrichment. Two typical bacteria *Escherichia coli* (*E. coli*) and *Mycobacterium smegmatis* were used as examples to validate the performance of the microfluidic chip. *Escherichia coli* is model of bacteria and widely used in many methodology tests. *Mycobacterium smegmatis* is the strain which had some similar traits with *Mycobacterium tuberculosis* and often applied in the study of tuberculosis for safety.

EXPERIMENTAL SECTION

Observation and Statistical Analysis of *E. coli* and *Mycobacterium smegmatis*. The bacteria sample collected by sedimentation was cultured at 37 °C for 24 h, then the number of colonies is calculated. The amount of captured (enriched) bacteria by microfluidic chip could be directly observed by microscope. Irradiated bacteria cells emit green fluorescence when excited by blue light, so once the bacteria cells are enriched, it could be observed immediately in the microfluidic chip under a fluorescence microscope. A laser scanning confocal microscope (model, Leica TCS SP5, Leica Geosystems, Germany, excitation at 488 nm) was used for observing *E. coli* and *Mycobacterium smegmatis*. The observation of uncaptured bacteria is based on bacteria culturing. Briefly, the bacteria suspension washed from the microchannel is transferred to a microcentrifuge tube and cultivated on the plates at 37 °C for 24 h. By adding antibiotics, only *E. coli* cells or *Mycobacterium smegmatis* cells used in this experiment can be cultivated, respectively. The numbers of bacteria is identified by using the dilution-plate counting method.

Bacteria Aerosol Particle Size (APS) Measurement. The particle size distribution of the bioaerosol generated by the aerosol generator (Figure 2A) was detected by APS (model 3321; TSI, Inc., St. Paul, MN). The sample mode of APS was the summed mode; sheath flow, 41 pm; sample flow, 11 pm; sample type, continuous; inlet pressure, 1000 Mbar; detection range, 0.5−20 μm. The initial concentration of *E. coli* bacteria suspension was 10^6 cell mL^{-1}. The aerosol generator was used to generate the bioaerosol for 2 min.

Microfluidic Chip Fabrication. The chips were fabricated following standard soft lithography.[39,44,45] Two pieces of the molds were both made from SU8 2025 photoresist, consistent with the patterns of the fluidic layer and herringbone layer. Two pieces of PDMS polymer plate casted from these two molds were assembled together precisely. Inlet and outlet holes were punched, and Teflon tubes were inserted for air/water input. The channel surface of PDMS microfluidic chip were sequentially washed by HCl (1.0% v/v), H_2O_2 (1.0% v/v), and water and dried with clean nitrogen before use.[46]

RESULTS AND DISCUSSION

Structure of the Microfluidic Device. The device consists of a microfluidic chip made from two pieces of polydimethylsiloxane (PDMS) plate and two plates of polymethyl methacrylate (PMMA) bonded to the upper and lower surfaces of the chip (Figure 1B). The two layers of PDMS are assembled together through thermal polymerization. Four screws at the four corners of the PMMA plates are used to assemble the two

dx.doi.org/10.1021/ac400590c | *Anal. Chem.* 2013, 85, 5255−5262

pieces of the PMMA plates and the double-layer PDMS chip together. The PDMS based microfluidic device is designed for capturing and enriching bacteria from the air. Figure 1B,C shows the layout and the photograph of a double-layer integrated microfluidic device for enrichment. It consists of an inlet, an outlet, and the inside enrichment channel. The inlet and outlet are designed for air/water input and output. The diameter of inlet hole and outlet hole are about 1.5 mm. The core capture and enrichment channel is 17.4 cm long, 600 μm wide, and 40 μm high. The enrichment channel is designed as an s-shaped zone and chaotic flow zone. The chaotic flow zone is made up of a row of staggered herringbones in order to create chaotic flow and get better bacteria capture efficiency. The inside channel surface of the microfluidic chip is modified to be hydrophyllic for better bacteria capture.[46]

Automated Enrichment System and Mechanism. Figure 2 illustrated the structure of the enrichment system.

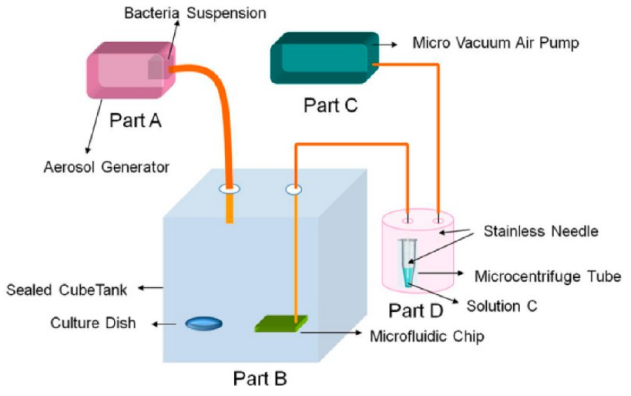

Figure 2. Illustration of the system to test the efficiency of the microfluidic device.

Part A is an aerosol generator (medical ultrasonic nebulizer, BEIERSI, BSW-2A, China) containing a certain concentration of bacteria suspension. Part B is a cube tank with a 125 L volume. There is a hole on the tank for a clean air supplement, and it is covered by a filter made by 16 layers of gauze. Part C is a microvacuum air pump (HARGRAVES) and prepared to draw the aerosol into the microfluidic chip. The flow rate can be adjusted from 1.0 to 12.0 mL min^{-1} when connected with the microfluidic chip. Part D is an airtight glass bottle with a 1.5 mL microcentrifuge tube inside, and the tube is half filled with resuspension solution.

As shown in Figure 2, one Teflon tube is connected with the airtight glass bottle through the stainless needle at the end (outside of the microcentrifuge tube). Another end of the tube is connected with the microvacuum air pump. Another Teflon tube connected with a stainless needle is immersed into the resuspension solution. The other end of this Teflon tube is connected to the enrichment microfluidic chip.

The brief bacteria enrichment mechanism is shown as following. First, a certain concentration of bacteria aerosol made by the aerosol generator (part A) enters the cube tank (part B). Under the vacuum by the micropump, the bacteria aerosol is drawn into the channels of the microfluidic chip. At the same time, a LB culture dish is placed in the tank as a parallel control (sedimentation method). Bacteria may be captured by adhering to the inside walls of microchannels in the chip. The uncaptured bacteria will pass through the chip and enter the resuspension solution and get collected there. After enrichment, 2 μL of buffer is loaded into the microchannel to wash the captured bacteria inside the microfluidic chip, and the solution is collected at the outlet for statistical analysis. In this experiment, three parallel bacteria samples were collected, including bacteria sample collected by the sedimentation method, bacteria sample captured by microfluidic chip, and bacteria collected by the suspension solution in the micro-centrifuge tube.

Particle Size Distribution of *E. coli* Bacteria Aerosol. Bacteria aerosol particles that exist in nature may be suspended as individual cells but are more likely to be attached to other particles, such as soil or leaf fragments, or found as agglomerates of many bacteria cells.[47−51] The actual measured diameter of bacteria aerosol were reported from smaller than 4 μm to larger than 18 μm,[51−53] though the individual bacteria are typically about 1 μm or less. Figure 3 shows an example size

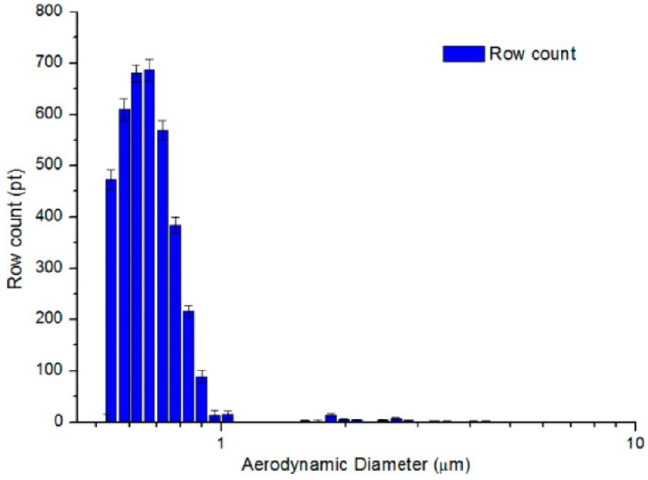

Figure 3. Raw particle counts of *E. coli* bacteria aerosol measured by APS (10^6cell mL^{-1} *E. coli* suspension).

distribution of the raw number of particles measured. This was measured by APS, in the aerosol generator sample generated in the first 2 min of aerosolization of 10^6 *E. coli* particles mL^{-1} of suspension. The sampling interval time was 1 min. It can be seen that the raw particle counts by APS was mainly less than 1 μm. Also, the peak value of the row count was about 700 cells when the aerodynamic diameter was 0.673 μm. There are also some particles in which the aerodynamic diameter is larger than 1 μm. This result showed that the bioaerosol particles generated by the medical ultrasonic nebulizer was similar to the literature report.[54,55]

Enrichment Efficiency. Enrichment efficiency is related to the contact chances between the bacteria in the aerosol and the inner walls of the microchannels inside the microchip. Because of the low Reynolds number, the steady laminar flow is dominant in microfluidic channels, which would limit the contact chance between the bacteria and channel surface. In order to break the laminar flow, the staggered herringbone structure is introduced inside the channel (Figure 1), which could induce vortex to boost the flow rotating and stretching.[56,57] The second drawing of Figure 1A shows the representative two sequential ridges of the staggered herringbone mixer (SHM) structure, and it has been demonstrated that this structure could change the centerline of channel from one region to the next, which could make rapid and efficient chaotic mixing from steady pressure-driven

dx.doi.org/10.1021/ac400590c | *Anal. Chem.* 2013, 85, 5255−5262

laminar flows in microchannels.[58] Consequently, the high bacteria enrichment efficiency is expected from this design.

In order to investigate the enrichment efficiency changing with time, enrichment analysis at 10 different experimental intervals, 0−60 min have been studied (Tables 1 and 2). The

Table 1. Enrichment of *E. coli* with Time in Microfluidic Chip

experimental time (min)	total no. of enriched bacteria (cfu)	total no. of unenriched bacteria (cfu)	enrichment efficiency (%)
0	0	0	0
9	947	0	100
12	6 800	0	100
15	122 860	0	100
18	160 000	0	100
21	216 600	0	100
24	304 000	0	100
27	340 000	0	100
30	469 600	0	100
60	440 000	30	99.9

Table 2. Enrichment of *Mycobacterium smegmatis* with Time in Microfluidic Chip

experimental time (min)	total no. of enriched bacteria (cfu)	total no. of unenriched bacteria (cfu)	enrichment efficiency (%)
0	0	0	0
9	116 500	15	99.99
12	124 000	12	99.99
15	133 000	18	99.99
18	153 000	32	99.99
21	182 000	29	99.98
24	199 000	27	99.99
27	208 000	93	99.96
30	372 000	93	99.98
60	405 000	99	99.98

microfluidic chip is placed in the sealed cube tank as illustrated in Figure 2. After a saturation of bacteria aerosol, the microvacuum air pump starts to work for a preset time. The bacteria aerosol is maintained in a saturated state to ensure that there are enough bacteria to get absorbed onto the microchannel. Experimental data of *E. coli* and *Mycobacterium smegmatis* enrichment efficiency are shown in Tables 1 and 2 respectively. The results show that the enrichment microfluidic chip is well capable of capturing *E. coli* and *Mycobacterium smegmatis* from aerosol. The total numbers of enriched bacteria increased as experimental time increases. No uncaptured *E. coli* bacteria are found from part D at the time interval from 0 to 30 min during our experiment, which made the enrichment efficiency about 100% at these time intervals. Uncaptured *E. coli* bacteria could only be detected until 60 min, at which, about 30 *E. coli* bacteria are found to flow through the microchannel. This number is extremely small compared with the total numbers of enriched bacteria at 60 min. The enrichment efficiency of *Mycobacterium smegmatis* is also more than 99.9%. It is clear that the designed microfluidic chip can capture *E. coli* bacteria and *Mycobacterium smegmatis* bacteria at very good efficiency from the aerosol and most of these bacteria can adhere to the inside walls of the microchannel.

During this experiment, the high enrichment efficiency is believed due to the high efficient chaotic flow by SHM structure. The SHM structure at the chaotic flow zone changes the airflow from steady laminar flow to chaotic flow and the aerosol flow is continuously twisted when passing through the microchannels, enhancing the contact opportunity between the bacteria and the surface of the microchannels. Moreover, the SHM structure can also increases the surface area of the microchannel to further improve the enrichment efficiency. Less repeating units would increase the flow rate, but it would increase the flee chance of the bacteria. Too many repeating units are likely to have the opposite effect. Given consideration of the time and the enrichment efficiency, 24 repeat units were adopted in the channel to balance the capture efficiency and enrichment time.

Detection of *E. coli* and *Mycobacterium smegmatis* under Laser Scanning Confocal Microscope. In this experiment, the microchannel is also examined under a confocal microscope to observe the way *E. coli* bacteria and *Mycobacterium smegmatis* are captured (Figure 4). Figure 4a−

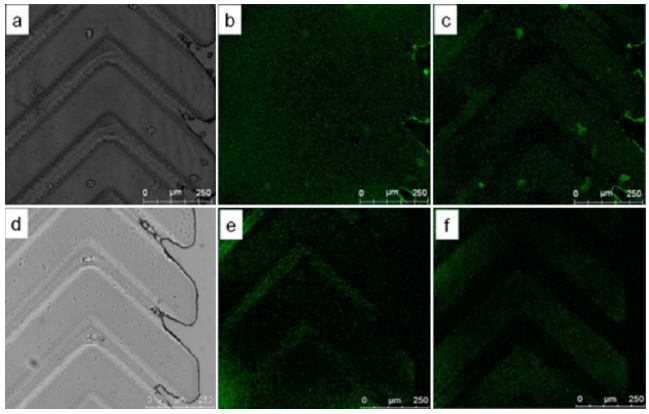

Figure 4. Visible and fluorescence image of microfluidic channels with bacteria inside (a−c) *E. coli*: (a) SHM image in visible range, (b) fluorescence image focused on the ridge plane of the SHM, and (c) fluorescence image focused on the groove plane of the SHM. (d−f) *Mycobacterium smegmatis*: (d) SHM image in visible range, (e) fluorescence image focused on the ridge plane of the SHM, and (f) fluorescence image focused on the groove plane of the SHM.

c and d−f show the laser scanning confocal microscopic images of *E. coli* and *Mycobacterium smegmatis* inside the microchannel, respectively. Aerosols are prepared from the original concentration suspension, 10^6 cell mL^{-1}. Bacteria cells, with green fluorescence, are clearly seen when exposed to blue light. Figure 4a,d shows the SHM image of in parts b,c and e,f in Figure 4, respectively, in visible light. Parts b and e of Figure 4, respectively, showed the way that the *E. coli* and *Mycobacterium smegmatis* bacteria adhered to the ridge of the SHM. Parts c and f of Figure 4, respectively, showed that the *E. coli* and *Mycobacterium smegmatis* adhered to the groove of the SHM. It is clear from Figure 4 that under the 10^6cell mL^{-1} condition, there were many *E. coli* and *Mycobacterium smegmatis* bacteria that could be identified in the microchannels. *E. coli* and *Mycobacterium smegmatis* could adhere to the groove as well as the ridge of the SHM. The ridge planes and the groove planes of the SHM have an equally good chance for *Mycobacterium smegmatis* to adhere. The function of the microfluidic chip to enrich the *E. coli* and *Mycobacterium smegmatis* bacteria is clearly illustrated.

dx.doi.org/10.1021/ac400590c | *Anal. Chem.* 2013, 85, 5255−5262

Fluorescence Detection of Bacteria along the Channel. The fluorescence of *E. coli* bacteria adhered along the channel from inlet to outlet was observed by a laser scanning confocal microscope (Figure 5). The channel connected with the inlet had strong fluorescence intensity (Figure 5a1). Fluorescence intensity decreased gradually along the channel. The image in parts b1 and c1 of Figure 5 were the fluorescence taken at the first $^1/_3$ section and the half-length place inside the channel, respectively. At the end of the herringbone structure (Figure 5d1) and the plain channel next to the outlet, no fluorescence was detected. It was clear that almost no bacteria reached this area, confirming the nearly 100% enrichment efficiency.

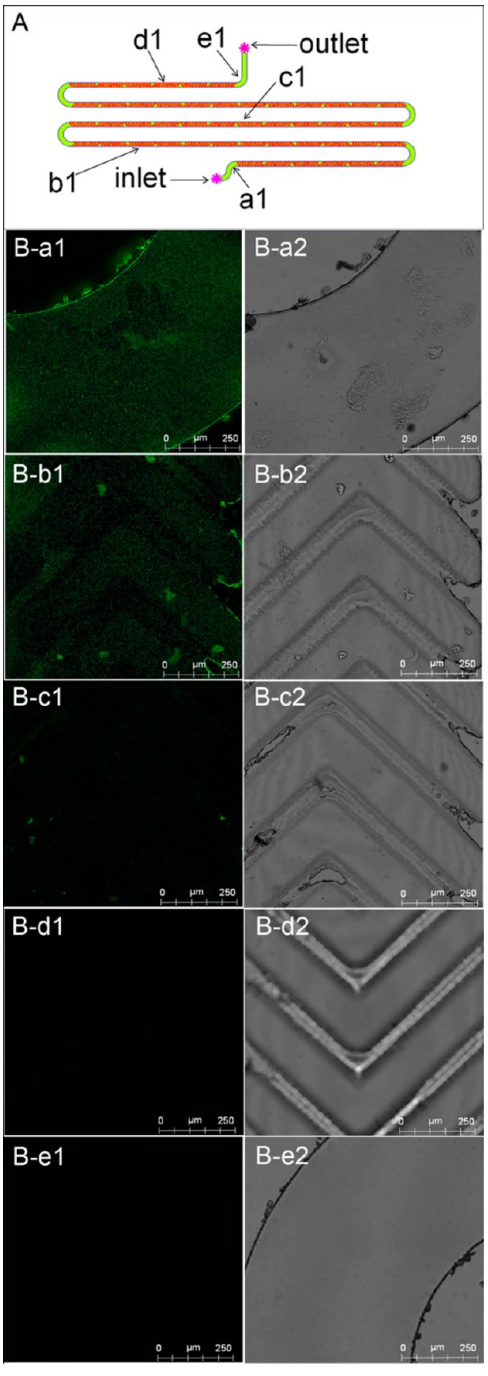

Figure 5. Fluorescence image of *E. coli* bacteria along the channel: (A) schematic of the locations, (B) a1,a2, channel connect to the inlet; b1,b2, herringbone structure at the first third section of the channel; c1,c2, herringbone structure at the half -length of the channel; d1,d2, herringbone structure at the end of the channel; e1,e2, channel connect to the outlet. Images a1, b1, c1, d1, and e1 were fluorescent images excited by blue light. Images a2, b2, c2, and d2 were visible images taken at the same places as the fluorescent images.

Detection Limit of *E. coli* and *Mycobacterium smegmatis* in Enrichment Microfluidic Chip. Figure 6A shows the number of *E. coli* bacteria collected by the enrichment microfluidic chip compared with the number of it collected by the plate sedimentation method. The results show that *E. coli* bacteria can be collected by an enrichment microfluidic chip at all the three different concentrations. In the same given time of 20 min, much more bacteria can be collected by the enrichment microfluidic chip compared with that collected by the plate sedimentation method. When the concentration of *E. coli* bacteria suspension was 10^5 cell mL^{-1}, there were 254 cells collected by the microfluidic chip, which is more than 4.53 times higher than that collected by the plate sedimentation method, 56 cells. When the concentration of *E. coli* bacteria suspension is 10^4cell mL^{-1}, there are still 130 units collected by the microfluidic chip, which was 4 times higher than that collected by the plate sedimentation method, 26 cells. Even there is only one strain detected by the traditional collected method when the concentration of *E. coli* bacteria suspension decreased to 10^3cell mL^{-1}, the microfluidic chip still could catch 56 bacteria cells, which is 55 times higher. When the 10^4cell mL^{-1} bacteria suspension is utilized for measurement, 130 *E. coli* bacteria captured by the microfluidic chip are

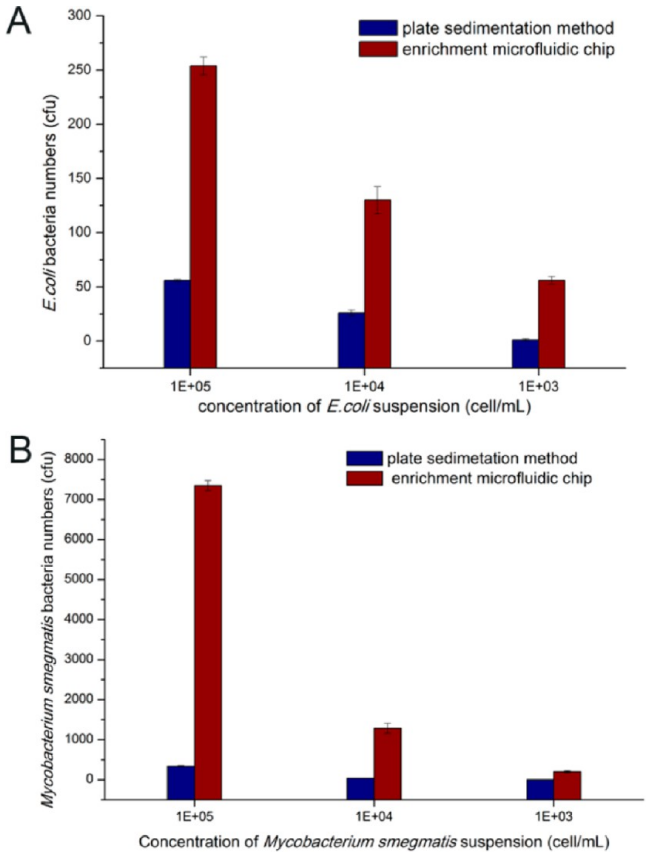

Figure 6. Capture of bacteria using the enrichment microfluidic chip and sediment plate: (A) *E. coli* and (B) *Mycobacterium smegmatis*.

dx.doi.org/10.1021/ac400590c | *Anal. Chem.* 2013, 85, 5255−5262

Table 3. Comparison between SHM Structure and Non-SHM Structure

structure	channel size	inlet/outlet diameter	flow rate	bacteria	enrichment time	efficiency (%)
SHM	(length × width × height)	1500 μm	4.4 mL min^{-1}	10^6 cell mL^{-1}	20 min	100
non-SHM	17.4 cm ×600 μm × 40 μm					65.6

enough for rapid detection methods, such as an ELISA based test (100 bacteria are enough for ELISA based tests as well as PCR based tests). Similar results are obtained from the test with *Mycobacterium smegmatis* though the *Mycobacterium smegmatis* is more viscid than *E. coli*, more difficult to collect. At the 10^5 cell mL^{-1} suspension concentration to prepare the bioaerosol, the microfluidic chip collected 7350 *Mycobacterium smegmatis* bacteria vs 340 by the sediment plate. At the 10^4cell mL^{-1} suspension concentration, the microfluidic chip collected 1289 bacteria vs 39 by the sediment plate. At the 10^3 cell mL^{-1} suspension concentration, the microfluidic chip collects 204 bacteria vs 1 by the sediment plate. In brief, the enrichment microfluidic chip cannot only collect *E. coli* and *Mycobacterium smegmatis* bacteria in a short time, but also the bacteria enrichment efficiency as well as the capture limit are much better than that of the plate sedimentation method.

Enrichment Efficiency Comparison between SHM Structure and Non-SHM Structure. In order to study the effects of the SHM structure on the enrichment efficiency of microfluidic chips, two types of microfluidic chip with/without the SHM structure were fabricated, and parallel enrichment experiments under the same conditions have been performed, which included channels size, flow rate, enrichment time, and concentration of bacteria in the aerosol (Table 3). The bacteria aerosol was maintained in the saturated state to ensure that there were enough bacteria to get absorbed onto the microchannel. The results show that the enrichment efficiency of the SHM structure microfluidic chip was higher than that of the non-SHM structure microfluidic chip. The enrichment efficiency of the SHM structure was 100% (about 2.3 × 10^5 cells enriched and no cells leaking out) and the efficiency of the non-SHM structure microfluidic chip was only about 65.6% (about 1.52 × 10^5 cells enriched and 7.97 × 10^4 cells leaking out). The results proved that the SHM structure was important for airborne bacteria enrichment. Former research had already demonstrated that the SHM structure could make the liquid rapidly with efficient chaotic mixing from steady pressure-driven laminar flows in the microchannels.[58] To our knowledge, this is the first time to apply this structure in airborne bacteria enrichment, and the effect was very obvious. Chaotic mixing provided more possibilities for bacteria to touch the inner wall of the microchannel.

The herringbone shape can induce chaotic flow when aerosol with airborne bacteria passes through the channel.[58] The existence of chaotic flow means vortexes are generated in the channel, creating more contact chance between the bacteria and channel inner walls. Numerical simulations have also been conducted to investigate the capture efficiency of bacteria inside the herringbone microfluidic channel as well as the corresponding air flow dynamics inside the channels. For the easy simulation, the particles at the inlet (left down corner) and their moving paths inside the channel are represented as lines of different color. Stop of the moving routine means positive capture. These particles are assumed as zero mass and a solid sphere structure at diameter 1 μm. Affirmative capture is upon direct contact between the particle and inner channel wall. As show in the Figure 7, the U channel containing two

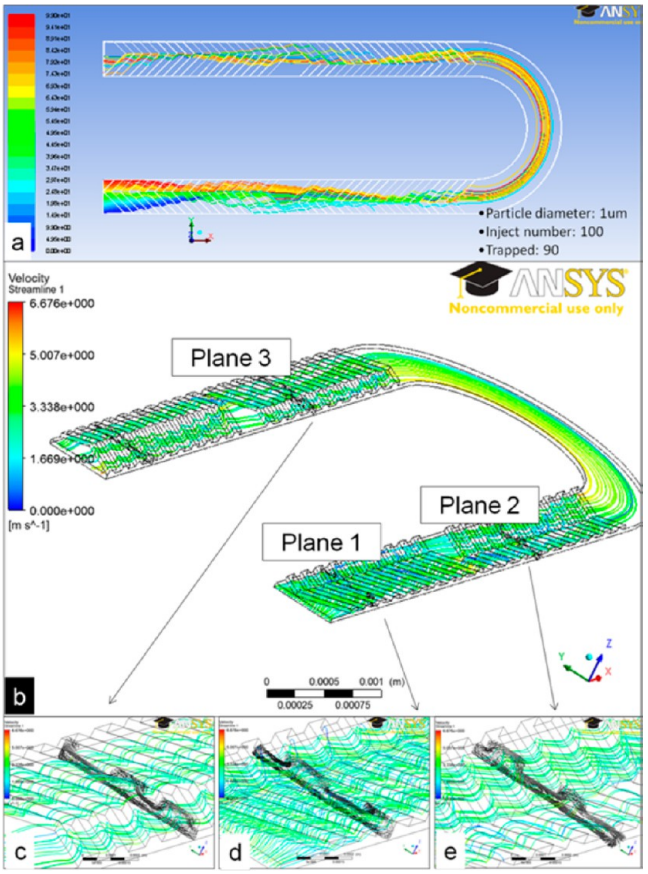

Figure 7. Numerical simulations of the capture efficiency of bacteria as well as the corresponding air flow dynamics inside the herringbone channels. (a) capture efficiency with loading 100 particles. Moving paths are represented by different colors: (b) flow dynamics inside the microfluidic channel; (c,d, and e) vortex flows and moving paths of particles at intersection planes 1, 2, and 3.

representive herringbone structures and a smooth curve channel are used for simulation. A total of 100 particles are loaded into the channel at a flow rate of 4.4 mL min^{-1}, and 90 of them are captured, while only 10 particles pass through the channel. These particles keep changing moving directions instead of the parallel manner at the inlet, due to the chaotic air flow carrying these particles. Intersections (planes 1, 2, and 3) are taken to show the flow dynamics at different positions. Instead of the common laminar flow inside the microfluidic channel, different vortex flow can be identified from these intersections, and vortex flows keep changing at different positions, due to the herringbone structure. Because of these changing vortex flows, particles inside the channel keep changing moving directions instead of parallel moving following the laminar flow in a smooth channel without the herringbone structure, obtaining more chances to hit the inner wall and getting captured. These simulation explained a high capture efficiency of the microfluidic chip. The capture efficiency is higher than that of the real experiments due to its strict

dx.doi.org/10.1021/ac400590c | *Anal. Chem.* 2013, 85, 5255−5262

postulations, such as zero mass, sphere structure and positive capture upon contact, and so on.

CONCLUSIONS

Herein an efficient microfluidic device for airborne bacteria capture and enrichment has been developed successfully. Two bacteria, *E. coli* and *Mycobacterium smegmatis*, have been utilized to validate the efficiency and capture limit of the device. The experimental results showed that capture efficiency and capture limit had been improved with this microfluidic device compared with the traditional method under the same conditions. The capture efficiency of the microfluidic chip reaches almost 100%, possibly due to the staggered herringbone structure of the microfluidic device.

Moreover, the detection limit of the microfluidic device is much lower than the plate sedimentation method. It can collect enough bacteria at a low aerosol concentration for a direct ELISA, loop-mediated isothermal amplification (LAMP) test, which is essential for rapid bacteria detection, especially compared with traditional bioaerosol collection techniques which need the downstream culturing or PCR amplification because of the relative high capture limit.

The microfluidic chip with/without SHM structure and non-SHM structure was made to investigate the effects of the herringbone structures on airborne bacteria capture efficiency. The enrichment efficiency of the microchannel with the SHM structure has reached about 100%, while that ratio reaches only 65.6% in channels without the SHM structure. Numerical simulations have been conducted to investigate the capture efficiency of bacteria inside the herringbone microfluidic channel as well as the corresponding air flow dynamics inside the channels. Simulation results as well as the experimental results both proved that the vortex chaotic flow created by the herringbone structure is the key of the high bacteria capture efficiency.

Different flow rates as well as different channel lengths on enrichment efficiency of the microfluidic chip were investigated (detailed in the Supporting Information). The results showed that the channel length and flow rate are both important factors for airborne bacteria enrichment. Taking enriched bacteria numbers and enrichment efficiency into consideration, channel length was set at 17.4 cm and the flow rate was set at 4.4 mL min^{-1} for better performance. Although about a 9−10 cm long channel would be enough for efficient capture of all the bacteria. A 17.4 cm channel is selected to ensure no bacteria is leaking.

The whole system consists of a pump, disposable microfluidic chip, and connection tubing, which is rigid and simple, perfect for field application, the hospital, or other airborne microorganisms' high-risk environment. The microfluidic chip is also very simple and easy to fabricate from plastics by molding. The device can be easily integrated with a fast detection module such as a test strip, ELISA test kit to form a complete pathogen analysis appliance. The whole system has the potential to become a crucial platform in biological and medical applications for rapid identification of pathogenic microorganisms and other particulate matter in the aerosol.

ASSOCIATED CONTENT

Supporting Information

Additional information as noted in text. This material is available free of charge via the Internet at http://pubs.acs.org.

AUTHOR INFORMATION

Corresponding Author

*E-mail: gsui@fudan.edu.cn (G.S.).

Author Contributions

[‖]W.J. and W.Z. contributed equally to this work.

Notes

The authors declare no competing financial interest.

ACKNOWLEDGMENTS

The authors thank for the funding support from NSFC (Grants 20975025 and 20807011), Cultivation Fund of the Key Scientific and Technical Innovation Project, Ministry of Education of China (Grant 708031), National Key Scientific Program (Grant 2009ZX10004-505), and Specialized Research Fund for the Doctoral Program of Higher Education (Grant SRFDP 20090071110006) and Shanghai Pujiang Support (Grant 09PJ1400900).

REFERENCES

(1) Senkpiel, K.; Kienast, E.; Herbst, M.; Ohgke, H. *Gefahrst. Reinhalt. L.* **1998**, *58*, 473−478.

(2) Glasgow, H. B.; Burkholder, J. M.; Schmechel, D. E.; Tester, P. A.; Rublee, P. A. *J. Toxicol. Environ. Health* **1995**, *46*, 501−522.

(3) Chen, Z.; Mauk, M. G.; Wang, J.; Abrams, W. R.; Corstjens, P. L. A. M.; Niedbala, R. S.; Malamud, D.; Bau, H. H. *Oral-Based Diagn.* **2007**, *1098*, 429−436.

(4) Dellinger, R. P.; Carlet, J. M.; Masur, H.; Gerlach, H.; Calandra, T.; Cohen, J.; Gea-Banacloche, J.; Keh, D.; Marshall, J. C.; Parker, M. M.; Ramsay, G.; Zimmerman, J. L.; Vincent, J. L.; Levy, M. M.; Surviving Sepsis Campaign, M. *Crit. Care. Med.* **2004**, *32*, 858−873.

(5) Larbcharoensub, N.; Aroonroch, R.; Kanoksil, W.; Leopairut, J.; Nitiyanant, P.; Khositseth, A.; Tangnararatchakit, K.; Chuansumrit, A.; Yoksan, S. *Southeast Asian J. Trop. Med. Public Health* **2011**, *42*, 1106−1112.

(6) Mattila, K. J.; Valtonen, V. V.; Nieminen, M. S.; Asikainen, S. *Clin. Infect. Dis.* **1998**, *26*, 719−734.

(7) Dellit, T. H.; Owens, R. C.; McGowan, J. E., Jr.; Gerding, D. N.; Weinstein, R. A.; Burke, J. P.; Huskins, W. C.; Paterson, D. L.; Fishman, N. O.; Carpenter, C. F.; Brennan, P. J.; Billeter, M.; Hooton, T. M. *Clin. Infect. Dis.* **2007**, *44*, 159−177.

(8) Hagan, K. A.; Reedy, C. R.; Uchimoto, M. L.; Basu, D.; Engel, D. A.; Landers, J. P. *Lab Chip* **2011**, *11*, 957−961.

(9) You, D. J.; Tran, P. L.; Kwon, H.-J.; Patel, D.; Yoon, J.-Y. *Faraday Discuss.* **2011**, *149*, 159−170.

(10) Boedicker, J. Q.; Li, L.; Kline, T. R.; Ismagilov, R. F. *Lab Chip* **2008**, *8*, 1265−1272.

(11) Lin, F. Y. H.; Sabri, M.; Erickson, D.; Alirezaie, J.; Li, D. Q.; Sherman, P. M. *Analyst* **2004**, *129*, 823−828.

(12) Pan, Y. L.; Boutou, V.; Bottiger, J. R.; Zhang, S. S.; Wolf, J. P.; Chang, R. K. *Aerosol Sci. Technol.* **2004**, *38*, 598−602.

(13) Dharmasiri, U.; Witek, M. A.; Adams, A. A.; Osiri, J. K.; Hupert, M. L.; Bianchi, T. S.; Roelke, D. L.; Soper, S. A. *Anal. Chem.* **2010**, *82*, 2844−2849.

(14) Ho, Y.-P.; Reddy, P. M. *Mass Spectrom. Rev.* **2011**, *30*, 1203−1224.

(15) Li, W.; Tse, F. L. S. *Biomed. Chromatogr.* **2010**, *24*, 49−65.

(16) Pybus, O. G.; Rambaut, A. *Nat. Rev. Genet.* **2009**, *10*, 540−550.

(17) Varshney, M.; Li, Y.; Srinivasan, B.; Tung, S. *Sens. Actuators, B: Chem.* **2007**, *128*, 99−107.

(18) Zhao, W.; Karp, J. M.; Ferrari, M.; Serda, R. *Nanotechnology* **2011**, *22*, 490201.

(19) Ren, P.; Jankun, T. M.; Belanger, K.; Bracken, M. B.; Leaderer, B. P. *Allergy* **2001**, *56*, 419−424.

(20) Pasanen, A. L. *Indoor Air* **2001**, *11*, 87−98.

(21) Aller, J. Y.; Kuznetsova, M. R.; Jahns, C. J.; Kemp, P. F. *J. Aerosol Sci.* **2005**, *36*, 801−812.

(22) Hogan, C. J.; Kettleson, E. M.; Lee, M. H.; Ramaswami, B.; Angenent, L. T.; Biswas, P. *J. Appl. Microbiol.* **2005**, *99*, 1422−1434.
(23) Jia, Y.; Fraser, M. *Environ. Sci. Technol.* **2011**, *45*, 930−936.
(24) Matrai, P. A.; Tranvik, L.; Leck, C.; Knulst, J. C. *Mar. Chem.* **2008**, *108*, 109−122.
(25) Lee, K. S.; Bartlett, K. H.; Brauer, M.; Stephens, G. M.; Black, W. A.; Teschke, K. *Indoor Air* **2004**, *14*, 360−366.
(26) Heidelberg, J. F.; Eisen, J. A.; Nelson, W. C.; Clayton, R. A.; Gwinn, M. L.; Dodson, R. J.; Haft, D. H.; Hickey, E. K.; Peterson, J. D.; Umayam, L.; Gill, S. R.; Nelson, K. E.; Read, T. D.; Tettelin, H.; Richardson, D.; Ermolaeva, M. D.; Vamathevan, J.; Bass, S.; Qin, H. Y.; Dragoi, I.; Sellers, P.; McDonald, L.; Utterback, T.; Fleishmann, R. D.; Nierman, W. C.; White, O.; Salzberg, S. L.; Smith, H. O.; Colwell, R. R.; Mekalanos, J. J.; Venter, J. C.; Fraser, C. M. *Nature* **2000**, *406*, 477−483.
(27) Pace, N. R. *Science* **1997**, *276*, 734−740.
(28) Qi, A.; Yeo, L.; Friend, J.; Ho, J. *Lab Chip* **2010**, *10*, 470−476.
(29) Yeo, L. Y.; Friend, J. R. *Biomicrofluidics* **2009**, *3*, 012002.
(30) Bhagat, A. A. S.; Hou, H. W.; Li, L. D.; Lim, C. T.; Han, J. *Lab Chip* **2011**, *11*, 1870−1878.
(31) Hur, S. C.; Mach, A. J.; Di Carlo, D. *Biomicrofluidics* **2011**, *5*, 022206.
(32) Yamamoto, S.; Watanabe, Y.; Nishida, N.; Suzuki, S. *J. Sep. Sci.* **2011**, *34*, 2879−2884.
(33) Li, Y. B.; Su, X. L. *J. Rapid Methods Autom. Microbiol.* **2006**, *14*, 96−109.
(34) Varshney, M.; Li, Y.; Srinivasan, B.; Tung, S.; Erf, G.; Slavik, M. F.; Ying, Y.; Fang, W. *Trans. ASABE* **2006**, *49*, 2061−2068.
(35) Yin, N. F.; Killeen, K.; Brennen, R.; Sobek, D.; Werlich, M.; van de Goor, T. V. *Anal. Chem.* **2005**, *77*, 527−533.
(36) Fu, Z.; Shao, G.; Wang, J.; Lu, D.; Wang, W.; Lin, Y. *Anal. Chem.* **2011**, *83*, 2685−2690.
(37) Park, S.; Zhang, Y.; Lin, S.; Wang, T.-H.; Yang, S. *Biotechnol. Adv.* **2011**, *29*, 830−839.
(38) Holmes, D.; Morgan, H. *Anal. Chem.* **2010**, *82*, 1455−1461.
(39) Liu, C. *Microfluid. Nanofluid.* **2010**, *9*, 923−931.
(40) Reisewitz, S.; Schroeder, H.; Tort, N.; Edwards, K. A.; Baeumner, A. J.; Niemeyer, C. M. *Small* **2010**, *6*, 2162−2168.
(41) Lim, E.; Tay, A.; Nicholson, A. G. *J. Thorac. Oncol.* **2012**, *7*, E42−E43.
(42) Jang, K.; Tanaka, Y.; Wakabayashi, J.; Ishii, R.; Sato, K.; Mawatari, K.; Nilsson, M.; Kitamori, T. *Biomicrofluidics* **2012**, *6*, 11.
(43) Loutherback, K.; D'Silva, J.; Liu, L. Y.; Wu, A.; Austin, R. H.; Sturm, J. C. *AIP Adv.* **2012**, *2*, 7.
(44) Chabert, M.; Viovy, J.-L. *Proc. Natl. Acad. Sci. U.S.A.* **2008**, *105*, 3191−3196.
(45) Whitesides, G. M.; Ostuni, E.; Takayama, S.; Jiang, X. Y.; Ingber, D. E. *Annu. Rev. Biomed. Eng.* **2001**, *3*, 335−373.
(46) Sui, G. D.; Wang, J. Y.; Lee, C. C.; Lu, W. X.; Lee, S. P.; Leyton, J. V.; Wu, A. M.; Tseng, H. R. *Anal. Chem.* **2006**, *78*, 5543−5551.
(47) Jones, A. M.; Harrison, R. M. *Sci. Total Environ.* **2004**, *326*, 151−180.
(48) Schwartz, J.; Coull, B.; Laden, F.; Ryan, L. *Environ. Health Perspect.* **2008**, *116*, 64−69.
(49) Reponen, T. A.; Gazenko, S. V.; Grinshpun, S. A.; Willeke, K.; Cole, E. C. *Appl. Environ. Microb.* **1998**, *64*, 3807−3812.
(50) Lighthart, B. *FEMS Microbiol. Ecol.* **1997**, *23*, 263−274.
(51) Shaffer, B. T.; Lighthart, B. *Microb. Ecol.* **1997**, *34*, 167−177.
(52) Tong, Y. Y.; Lighthart, B. *Aerosol Sci. Technol.* **1999**, *30*, 246−254.
(53) Wang, C. C.; Fang, G. C.; Lee, L. *Toxicol. Ind. Health* **2007**, *23*, 133−139.
(54) Tobias, H. J.; Schafer, M. P.; Pitesky, M.; Fergenson, D. P.; Horn, J.; Frank, M.; Gard, E. E. *Appl. Environ. Microb.* **2005**, *71*, 6086−6095.
(55) Despres, V. R.; Huffman, J. A.; Burrows, S. M.; Hoose, C.; Safatov, A. S.; Buryak, G.; Frohlich-Nowoisky, J.; Elbert, W.; Andreae, M. O.; Poschl, U.; Jaenicke, R. *Tellus B.* **2012**, *64*, 58.
(56) Kee, S. P.; Gavriilidis, A. *Chem. Eng. J.* **2008**, *142*, 109−121.
(57) Du, Y.; Zhang, Z.; Yim, C.; Lin, M.; Cao, X. *Biomicrofluidics* **2010**, *4*, 024105.
(58) Stroock, A. D.; Dertinger, S. K. W.; Ajdari, A.; Mezic, I.; Stone, H. A.; Whitesides, G. M. *Science* **2002**, *295*, 647−651.